

Aerial manipulation robot composed of an autonomous helicopter and a 7 degrees of freedom industrial manipulator

K. Kondak¹, F. Huber¹, M. Schwarzbach¹, M. Laiacker¹, D. Sommer¹, M. Bejar² and A. Ollero^{3,4}



Fig. 1: First experimental platform for aerial manipulation with a 7DoF industrial manipulator based on a main-tail-rotor helicopter.

Abstract—This paper is devoted to a system for aerial manipulation, composed of a helicopter and an industrial manipulator. The usage of an industrial manipulator is motivated by practical applications which were identified in different cooperation projects with the industry. We address the coupling between manipulator and helicopter and show that even in case when we have an ideal controller for manipulator and a high-performance controller for helicopter, an unbounded energy flow can be generated by internal forces between helicopter and manipulator if both controllers are used independently. To solve this problem we propose a new kinematical coupling for control by introducing an additional manipulation DoF realized by helicopter rotation around its yaw axis. The new experimental setup and required modifications in the manipulator controller for this purpose are described. Further, we propose dynamical coupling which is implemented by modification of the helicopter controller feeding the interaction force/torque, measured between manipulator base and fuselage, directly to the actuators of the rotor blades. At the end, we present experimental results for aerial manipulation and their analysis.

I. INTRODUCTION

Aerial manipulation is the natural evolution of mobile manipulation towards the possibility to move a manipulator base free in 3D. The new applications for aerial manipulation as inspections and installations on sites with a difficult access (offshore facilities or contaminated areas) have already raised interest of companies and public institutions. To be able to work with the existing industrial equipment, e.g. installation of inspection robots, a manipulator payload of at least 10 kg as well as advanced manipulation capabilities are required. This motivated us to work on a system for aerial manipulation composed of a helicopter and an industrial manipulator.

Fig. 1 shows the structure of the system. It is composed of three main components: a flying platform, a manipulator rigidly mounted on the fuselage and a sensor system, in our case a vision system, for localization and tracking of the object to be manipulated. We consider the following general simplified mission: navigation to the specified target area using GPS, activation of the sensor system for object tracking, approaching the object using data from the camera system, hovering very closely to the object and perform a manipulation.

Progress in research related to aerial manipulation was already shown by some authors [1]–[6]. In most of these interesting concepts, a simple manipulation device with a low-complexity gripper was used.

The control of the system shown in Fig. 1 is complicated due to a strong dependence between orientation and translation by a helicopter. The lifting force of the helicopter is perpendicular to the main rotor plane. The translation is controlled by setting the desired orientation of the main rotor plane and the magnitude of the lifting force. The movement of the attached manipulator changed the helicopter orientation and therefore its position which leads to further movement of the manipulator aimed at keeping the end-effector at the desired position relative to the environment.

The control approach based on a complete model of the whole system is problematic due to the model complexity. There are many couplings in the system and it should be investigated, which of them should be compensated, and which feedback loops should be used for that.

The calculations and the first experiments show that the inertial forces, generated by manipulator movement, have a negligible influence on helicopter. A significant influence is exerted by changing the position of the CoG (center of gravity) of the manipulator and as a result of interactions between endeffector and environment. The changes of the manipulator CoG position influence helicopter orientation and translation of the whole system as explained above.

We started to develop a solution for control of an aerial manipulation system using a scheme with independent controllers for helicopter and manipulator. Each of these systems has been subject to extensive research (helicopter much less than manipulator) and controllers for them are available. We have been investigating different types of couplings between the manipulator and the helicopter and have been introducing couplings in the control scheme one by one. The experimental work which complements theoretical investigations and computer simulations is essential for this type of systems. In our previous work [6], [7] we have shown that, due to

¹German Aerospace Center (DLR), Oberpfaffenhofen, GERMANY

²University Pablo de Olavide, Seville, SPAIN

³University of Seville, Seville, SPAIN

⁴Center for Advanced Aerospace Technologies (CATEC), Seville, SPAIN

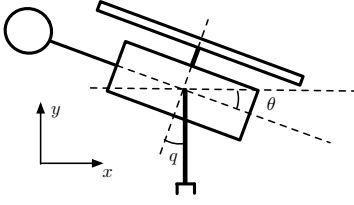


Fig. 2: Simplified system composed of a helicopter and one link manipulator moving in xy-plane

the phase shift of 90° between torques and angular rates on a spinning rotor, a helicopter with a manipulator can generate diverging cyclic movements, called phase cycles, if the manipulator tries to keep its end-effector at fixed position relative to the environment. In this work, we show that also without phase cycles, an increasing energy flow between the helicopter and the manipulator can be generated and make the whole system unstable, even in case of an ideal manipulator and a high-performance helicopter controller, sec. II. To reduce or even to eliminate this new effect, we propose to introduce an additional kinematical coupling into the control scheme by extending a 7-DoF manipulator with an additional rotational axis realized by rotation of the helicopter around its yaw axis, sec. III. In sec. IV, we introduce a dynamical coupling into the control scheme by modification of a helicopter controller. In sec. V we present and analyze the experimental results obtained with the setup in Fig. 1.

II. GENERAL CONSIDERATIONS TO DYNAMICAL COUPLING BETWEEN HELICOPTER AND MANIPULATOR

Let us consider a simplified system composed of a helicopter and an one-link manipulator, s. Fig. 2. The manipulator is attached to the center of mass of the helicopter. Its state is described by angle q and angular rate $u = \dot{q}$. The state of the helicopter is given by two coordinates x, y , angle θ , velocities $v_x = \dot{x}$, $v_y = \dot{y}$ and by angular rate $\omega = \dot{\theta}$.

We assume that the main rotor of a helicopter can generate the lifting force F , which is perpendicular to the main rotor plane, and torque T , directed perpendicular to the plane xy . F and T will be considered as inputs of the helicopter. We will consider an ideal controller for the manipulator which is able to generate in joint q desired angular rate u instantaneously. u will be considered as an input for the manipulator.

The dynamical eqs. of motion for the whole system are:

$$\begin{aligned} 0 &= -l m_l \cos(\theta + q) \dot{\omega} + l m_l \sin(\theta + q) (\omega + u) \quad (1) \\ &\quad - F \sin(\theta) - (m_h + m_l) \dot{v}_x \\ 0 &= -l m_l \sin(\theta + q) \dot{\omega} - l m_l \cos(\theta + q) (\omega + u) \quad (2) \\ &\quad + F \cos(\theta) - (m_h + m_l) \dot{v}_y - g(m_h + m_l) \\ 0 &= -l m_l g \sin(\theta + q) - l m_l \cos(\theta + q) \dot{v}_x \quad (3) \\ &\quad - l m_l g \sin(\theta + q) \dot{v}_y \\ &\quad + T - (I_h + I_l + m_l l^2) \dot{\omega} \end{aligned}$$

If we consider the same helicopter without manipulator ($m_l = 0$) the dynamical eqs. will be:

$$0 = -F \sin(\theta) - m_h \dot{v}_x \quad (4)$$

$$0 = F \cos(\theta) - m_h \dot{v}_y - g m_h \quad (5)$$

$$0 = T - I_h \dot{\omega} \quad (6)$$

Comparing the corresponding eqs. in both systems, we can see the interaction forces between the helicopter and the manipulator. So comparing the eq. (1) with eq. (4) we can see the interaction force $F_{int} = f_1 + f_2$ acting along x -axes between the helicopter and the manipulator with:

$$\begin{aligned} f_1 &= -l m_l \cos(\theta + q) \dot{\omega} \\ f_2 &= l m_l \sin(\theta + q) (\omega + u)^2 \end{aligned}$$

The energy flow between the helicopter and the manipulator due to F_{int} can be described by a port or couple $\langle F_{int}, v_x \rangle$. The corresponding total amount of energy inserted into the system, due to interaction between helicopter and manipulator, can be calculated with:

$$H = \int_{t=0}^{t=\tau} F_{int} v_x dt = \int_{t=0}^{t=\tau} f_1 v_x dt + \int_{t=0}^{t=\tau} f_2 v_x dt \quad (7)$$

Showing that $\lim_{\tau \rightarrow \infty} H = C < \infty$, or that after some time the helicopter receives from the manipulator an arbitrary small amount energy, we can conclude that the system composed of the helicopter with the manipulator is stable. Bellow we will show that H in (7) can be bounded by a constant if the gains of independent controllers for helicopter and manipulator satisfy some condition, which means that the whole system can be controlled by means of an independent controller for the helicopter and for the manipulator.

We analyze the first term in (7):

$$\int l m_l \cos(\theta + q) \dot{\omega} v_x dt \leq \kappa \int \dot{\omega} v_x dt \quad (8)$$

The helicopter controller keeps the helicopter in the equilibrium state $x^* = 0$. Having a position error, the position loop of the helicopter controller calculates a desired acceleration in order to decrease this error. The desired acceleration is recalculated to the desired lifting force F and helicopter orientation θ using eqs. (4,5):

$$\theta = \arcsin \left(-\dot{v}_x / \sqrt{\dot{v}_x^2 + (g + \dot{v}_y)^2} \right)$$

Taking into account that for reasonable flight envelop $\dot{v}_y \ll g$ as well as that $\arcsin(\alpha) \approx \alpha$ and that $\dot{v}_x = -k_v v_x$, we have:

$$\begin{aligned} \theta &= -k_v v_x / \sqrt{(k_v v_x)^2 + g^2} \\ \omega &= \frac{k_v^3 v_x^2 \dot{v}_x}{(g^2 + k_v^2 v_x^2)^{3/2}} + \frac{k_v \dot{v}_x}{(g^2 + k_v^2 v_x^2)^{1/2}} \end{aligned}$$

Transforming the right side of eq. (8) and inserting the last formula for ω we have:

$$\begin{aligned} \int \dot{\omega} v_x dt &= \omega v_x - \int \omega \dot{v}_x dt \\ &= -g^2 k_v \left[\int \frac{k_v^2 v_x^2}{(g^2 + k_v^2 v_x^2)^{3/2}} dt \right. \\ &\quad \left. + \frac{k_v v_x^2}{(g^2 + k_v^2 v_x^2)^{3/2}} \right] \end{aligned} \quad (9)$$

This function is negative definite and its derivative

$$\frac{g^2 k_v^3 v_x^2 (g^2 - 2k_v^2 v_x^2)}{(g^2 + k_v^2 v_x^2)^{5/2}}$$

is positive definite if

$$g^2 - 2k_v^2 v_x^2 > 0$$

With an assumption that $v_x \leq v_{max}$, which is not restrictive from the practical point of view, we get the condition for the gain in the outer loop of a helicopter controller:

$$k_v < \frac{g}{v_{max} \sqrt{2}} \quad (10)$$

We have shown that satisfying condition (10), the first term in eq. (7) for total energy insertion is bounded. With our assumption of a perfect controller for the manipulator, the second term in eq. (7) could be made bounded, because controlling q in such a way that its desired value is $-\theta$ (manipulator link is pointed perpendicular downwards), we could make $\sin(\theta + q)$ as close to zero as needed. Therefore, we haven shown that satisfying the condition (10) for the gain in the outer loop of the helicopter controller, we can make the system composed of a helicopter and manipulator with independent controllers stable.

From the presented analysis of this simple example, two conclusions can be made. First, an independent control of a manipulator and a helicopter induces energy flow between these two subsystems, which could lead to the instability of the whole system even if we have a perfect controller for the manipulator. Second, having an ideal manipulator controller, the gain in the outer loop of the helicopter controller should not be increased to its maximal possible value (given by the saturation of a helicopter), but should be reduced to some value in order to bind energy flow between the helicopter and the manipulator, caused by dynamical interaction between these two systems. It means that even having a high-performance controller for the helicopter, it could be difficult to utilize the available performance, and the helicopter will not be able to fly or hover precisely enough for a particular manipulation task.

Using this results, we decided to introduce kinematical and dynamical coupling in the control scheme which are described in the next sections.

III. MANIPULATOR CONTROL, KINEMATICAL COUPLING

As it could be shown in simulation and as it is verified in flight experiments presented in sec. V, the position changing

of the manipulator CoG is the main factor influencing the helicopter movement. The dynamical component is negligible due to a relatively slow motion of the manipulator (safety restrictions for experiments). The idea of the proposed kinematical coupling is to minimize the influence on the helicopter from the manipulator preventing the motion of the manipulator CoG as much as possible. In an ideal case, the manipulator CoG would be fixed in a fuselage frame but, as it will be discussed later, even a restriction of CoG movement in one plane or along an axis contributes to the performance of the whole system significantly.

In order to have six DoF in end-effector and to restrict the movement of manipulator CoG a redundant manipulator has to be used. We use a 7-DoF Light Weight Robot (LWR) for manipulation, which allows us to implement complex control strategies like impedance control, see e.g. [8]. The impedance control is one of the suitable control concepts, because it gives the manipulator an active elasticity and a possibility to reduce the interaction force on the fuselage in case of a contact. Especially by an undesired collision, the manipulator can react with a preset stiffness and absorb a part of the impact.

For the manipulation task, the motion is defined by a desired Cartesian position \mathbf{x}_d . With the impedance control and an adequate trajectory interpolation, the end-effector of the manipulator is pulled to the desired position by a virtual spring damper system.

Due to the redundancy, we do not have a completely defined configuration of the robot joints for a given position and orientation of end-effector. Thus, a null-space strategy must be designed. This opens up the possibility for additional conditions e.g. the aforementioned CoG control. This control strategy will be outlined below.

The Cartesian impedance control consists of an underlying joint torque controller with the desired torque vector $\boldsymbol{\tau}_d$ as input. The desired torque is given by

$$\boldsymbol{\tau}_d = \boldsymbol{\tau}_{d, Cart} + \boldsymbol{\tau}_{d, NSp} + \mathbf{g}(\mathbf{q}) \quad (11)$$

with $\boldsymbol{\tau}_{d, Cart}$ as the Cartesian impedance controller torque only affecting the end-effector and $\boldsymbol{\tau}_{d, NSp}$ for null-space motion of the manipulator. In order to reach the task goal $(\mathbf{x}_d, \dot{\mathbf{x}}_d)$, $\boldsymbol{\tau}_{d, Cart}$ is designed as

$$\boldsymbol{\tau}_{d, Cart} = \mathbf{J}_q^T (\mathbf{K}_x (\mathbf{x}(\mathbf{q}) - \mathbf{x}_d) + \mathbf{D}_x (\dot{\mathbf{x}}(\mathbf{q}) - \dot{\mathbf{x}}_d)) \quad (12)$$

with the manipulators Jacobian $\mathbf{J}(\mathbf{q})$, the current Cartesian end-effector position $\mathbf{x}(\mathbf{q})$ and velocity $\dot{\mathbf{x}}(\mathbf{q})$. \mathbf{K}_x and \mathbf{D}_x are positive definite matrices for the desired stiffness and damping. The desired Cartesian position \mathbf{x}_d and velocity $\dot{\mathbf{x}}_d$ are provided by the visual tracking. Furthermore equation (11) includes a gravity compensation term $\mathbf{g}(\mathbf{q})$. We get the actual gravitation from the on-board attitude sensors.

The desired null-space behavior can be described as a force \mathbf{f}_{CoG} acting on the forth joint (elbow joint) trying to pull the manipulator in a configuration that has the CoG of the manipulator as close as possible to a desired position in order to prevent its motion. As mentioned before, in an ideal case, the movement of CoG would be prevented completely.

The relationship between the force \mathbf{f}_{CoG} and the torque $\boldsymbol{\tau}_{CoG}$ can be written as

$$\boldsymbol{\tau}_{CoG} = \mathbf{J}_4^T(\mathbf{q})\mathbf{f}_{CoG} \quad (13)$$

with the manipulators Jacobian $\mathbf{J}_4(\mathbf{q})$ at the forth link.

In [6], [7] we have shown, that non-restricted movement of CoG can induce diverging oscillations of the whole system. The restriction of CoG movement to the lateral plane makes this oscillations impossible. For realization of this restriction, we used one DoF of the manipulator. In this case, the force in (13) is proportional to the distance $\|\mathbf{d}_{P,CoG}\|$ between the CoG \mathbf{r}_{CoG} and a vertical plane P and has the direction of $\mathbf{d}_{P,CoG}$

$$\mathbf{f}_{CoG} = \mathbf{f}_{CoG}(\mathbf{d}_{P,CoG}, \|\mathbf{d}_{P,CoG}\|). \quad (14)$$

The distance vector $\mathbf{d}_{P,CoG}$ is

$$\mathbf{d}_{P,CoG} = \frac{\mathbf{n}_{des}^T \mathbf{r}_{CoG} - \mathbf{n}_{des}^T \mathbf{p}}{\|\mathbf{n}\|} \mathbf{n}_{des} \quad (15)$$

with the normal \mathbf{n}_{des} and an arbitrary point \mathbf{p} in the plane P . \mathbf{f}_{CoG} tries to keep the CoG as close to the plane P as possible. This control scheme was implemented and tested in flight experiments presented in sec. V.

As shown in sec. II, even in case of a movement of CoG in one plane where phase cycles can not appear, the whole system can become unstable. Considering this fact, we propose a new hardware setup for aerial manipulation, shown in Fig. 3. In contrast to the setup shown in Fig. 1, the first axis of the manipulator is not parallel to the yaw axis of a helicopter, see frames O and H in Fig. 3. This allows us to realize an 8-DoF manipulator using helicopter yaw axis as additional rotational joint. Please note that the yaw angle of helicopter can be controlled in hovering state very precisely compared to other axes of the helicopter. The yaw controller can run using modern actuators with up to 300Hz. Using two DoF, the CoG movement can be restricted to a yaw axis of the helicopter. In an ideal case, this strategy will eliminate the influence of the manipulator on the helicopter, if the end-effector does not have a contact with the environment. To calculate the controls, the manipulator Jacobian $\mathbf{J}_4(\mathbf{q})$ in (13) is extended by an additional joint and the distance vector $\mathbf{d}_{P,CoG}$ in (14) is calculated as a distance to the yaw axis.

In both presented cases for CoG movement control, the vector $\boldsymbol{\tau}_{CoG}$ has to be projected into the null-space in order to prevent interferences with the end-effector control. A sufficient mapping is given by

$$\boldsymbol{\tau}_{d,NSp} = \left(\mathbf{I} - (\mathbf{J}(\mathbf{q})^+ \mathbf{J}(\mathbf{q}))^T \right) \boldsymbol{\tau}_{CoG} \quad (16)$$

where \mathbf{I} is the identity matrix and $\mathbf{J}(\mathbf{q})^+$ the pseudo-inverse (Moore-Penrose) of the manipulators Jacobian $\mathbf{J}(\mathbf{q})$, see e.g. [9].

IV. HELICOPTER CONTROL, DYNAMICAL COUPLING

We propose to realise the dynamical coupling by feeding the measured resultant force and the torque between the

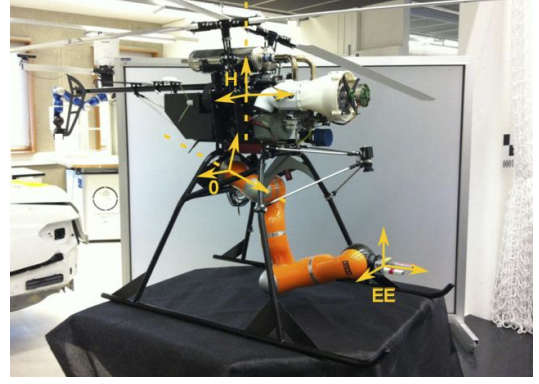


Fig. 3: Flettner helicopter with mounted LWR. Coordinate systems illustrate the realization of a manipulation device with 8 DoF.

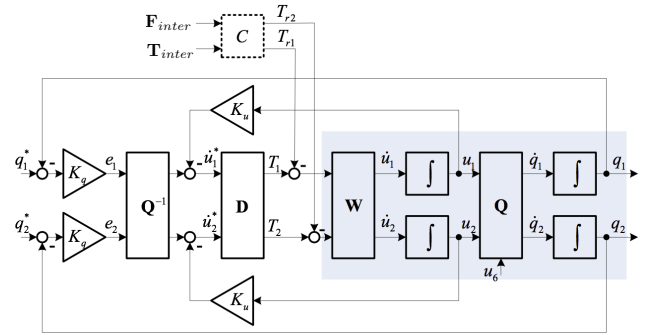


Fig. 4: Scheme for the orientation control

manipulator and the fuselage directly to the actuators of the main rotor blades. We developed a similar helicopter control scheme for load transportation system based on autonomous helicopters [10].

The scheme for the control of roll and pitch angles $q_{1,2}$ for a helicopter is shown in Fig. 4. Without dashed block C , this scheme corresponds to the controller for a helicopter without manipulator. The controller is composed of blocks \mathbf{Q}^{-1} , \mathbf{D} and two feedback loops with gains K_u , K_q for rotation speeds $u_{1,2}$ and orientation angles $q_{1,2}$ respectively. The rotational dynamics of a helicopter are represented in Fig. 4 by the block \mathbf{W} . The controller block \mathbf{D} decouples the plant between torques $T_{1,2}^{MR}$ generated by the main rotor, and $u_{1,2}$. This orientation controller shows a good performance and robustness in simulation and real flight experiments with different types of helicopters as we have shown in [10], [11].

The rotational dynamics of a helicopter coupled to the environment by means of a manipulator are strongly influenced by the motion of the whole system. To account for this influence, block \mathbf{D} should be replaced by the inverse rotational dynamics $\tilde{\mathbf{D}}$ not of a single helicopter, but of the whole system (considering both, the rotation and translation of each system component). The simulation experiments have shown that, in contrast to the case of a helicopter without a manipulator, the orientation controller with inverse block $\tilde{\mathbf{D}}$ is quite sensitive to variation of the system parameters (5% variation could be critical). To overcome this problem,



Fig. 5: Movement of the manipulator during the grasping task.

we proposed to use a force/torque measurement between manipulator and fuselage. The measured force \mathbf{F}_{inter} and torque \mathbf{T}_{inter} , will be used to calculate the influence on the rotational dynamics of the helicopter from the manipulator and environment. This influence on orientation controller is expressed by means of the torque $\mathbf{T}_r = \mathbf{F}_{inter} \times \mathbf{p}_{m-cm} + \mathbf{T}_{inter}$, where \mathbf{p}_{m-cm} is the position vector connecting sensor attachment point m and CoG of the system. The resulting orientation controller is composed of the orientation controller for a helicopter without a manipulator and the compensator block \mathbf{C} , see Fig. 4, where \mathbf{T}_r is calculated and subtracted from torques calculated in \mathbf{D} . The usage of the compensator \mathbf{C} has the following main advantages: the closed loop system becomes very robust against variation of system parameters/disturbances and the orientation controller for such a complicated system becomes quite simple.

There are two reasons for the robustness of the proposed orientation controller: first, the actual influence of the manipulator on the fuselage is measured through \mathbf{F}_{inter} , \mathbf{T}_{inter} and, therefore, the compensation becomes independent from the parameters and state of the manipulator. Second, as long as the orientation of the helicopter is known, the calculated compensation torque is always in the correct phase. It should be mentioned, that the bandwidth of torque generation on the main rotor of a helicopter is limited usually to 20–40Hz, so that the influence on the helicopter can not be compensated completely, even if the measurement is perfect.

V. EXPERIMENTAL RESULTS

The experiments were performed with the setup based on main-tail-rotor helicopter shown in Fig. 1 with the total takeoff weight of 120 kg, see [7] for more details about the setup. In the experiments, the behavior of the whole system performing a simplified manipulation task, as described in sec. I, was investigated. The helicopter had to fly to a specified position by means of GPS. At this position, the vision system for object recognition and tracking was activated. The helicopter went close to the object. The manipulator compensated the movement of the helicopter and grasped the object. Fig. 5 shows a sequence of pictures for the last phase

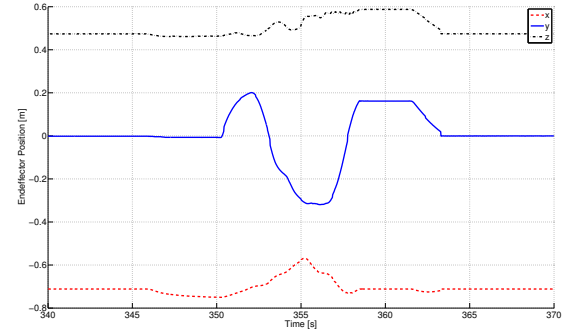


Fig. 6: Movement of the end-effector in the coordinate system, fixed on the manipulator base

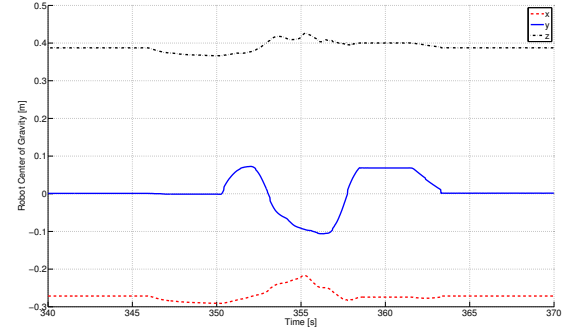


Fig. 7: Movement of the CoG in the coordinate system, fixed on the manipulator base

of the grasping. After grasping the object, the manipulator pulled the pole out of the fixing. During the pulling out, the pole was jammed in the fixing and caused a force interaction between the system and the environment.

In Fig. 6 and 7, the movement of the end-effector and CoG of the manipulator are shown. In both cases, the movement is given in the coordinate system fixed on manipulator base. As we can see in Fig. 6, the end-effector had to perform relatively large movements to compensate the displacement in y -direction. In Fig. 7 we can see the corresponding movement of CoG. The implemented manipulator controller tried to prevent the motion of CoG along the y -direction by mapping the corresponding torques into the null-space according to eq. (16). When approaching the object, one axis of the wrist joint was almost degenerated, so that the compensation of the CoG moment was possible only to some extent. This shows flexibility of the manipulator control scheme, which works even during approaching a degenerated configuration of the manipulator. In Fig. 7 and 6, we can see that a movement of the CoG in y -direction induced the disturbance of helicopter in x -direction which is compensated by the manipulator. This behavior is inherent to the aerial manipulation systems based on main-tail-rotor helicopters and was described using mathematical models in [6], [7]. If in such situation the system has enough time for movement, diverging phase cycles could appear.

In Fig. 8, joint torques are shown. In the time period

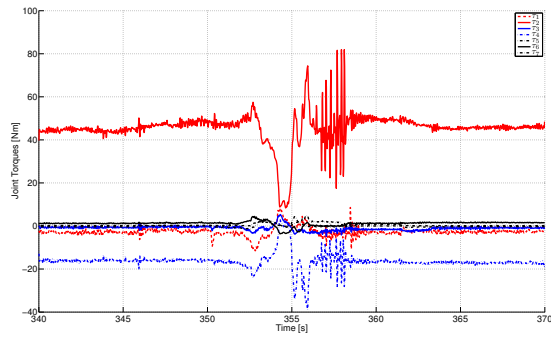


Fig. 8: Joint torques

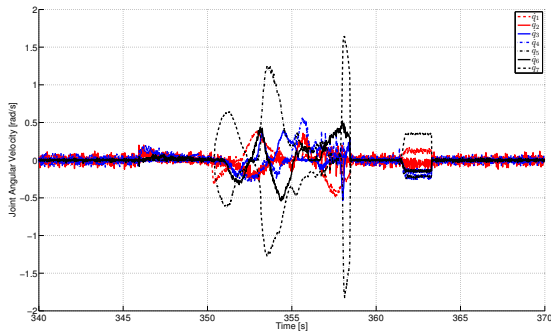


Fig. 9: Joint velocities

between 353 and 356 sec., the manipulator is pulling the jammed pole, and there is an interaction between the system and the environment. Interesting is also the time period between 357 and 358, where we see vibrations in the joints. In this time period, the manipulator has reached a virtual protection wall and slid on it. The control system was stopping and releasing the manipulator motion which caused this vibrations in joint torques.

In Fig. 9 the joint velocities are shown. The significant velocities corresponding to the black lines, are velocities for joints in the wrist. These axes do not move significant masses, so that their contribution to inertial forces is small. The velocities in other joints are small, therefore, the influence of the manipulator on the helicopter is exerted mainly by the current position of the manipulator CoG.

Fig. 10 shows filtered angular rates of the helicopter fuselage. In the time period between 350 and 360 sec., where the manipulator moved significantly, we see a correlation between angular rates along x and y axes. This shows the coupling between two axes of the helicopter as was explained above for Fig. 6 and 7.

VI. CONCLUSIONS

In this paper we presented further analysis of a world-wide first system for aerial manipulation composed of a helicopter and a fully actuated serial industrial manipulator. We have shown that for an independent control of the manipulator and the helicopter, an enhancement of the manipulation

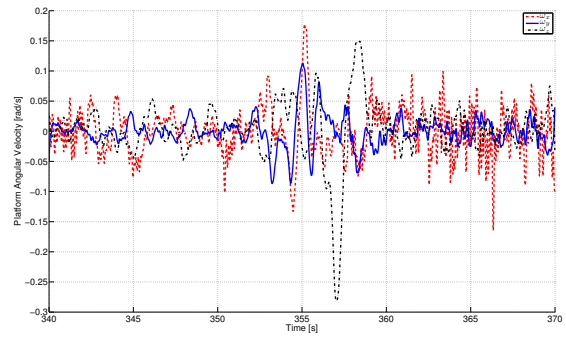


Fig. 10: Angular rates of the helicopter in the helicopter fixed frame

performance by increasing the helicopter controller gain could lead to an unstable system even in case of an ideal controller for a manipulator and a not saturated helicopter system. We proposed a control scheme for kinematical and dynamical coupling between two controllers. To increase the performance of the kinematical coupling, we suggested to use yaw axis of a helicopter as an additional axis of a manipulator. The presented experiments show that at least simple manipulation tasks are possible with the proposed setup. The analysis of the recorded logdata validates assumptions about the system behavior made from mathematical investigations.

REFERENCES

- [1] D. Mellinger, Q. Lindsey, M. Shomin, and V. Kumar, "Design, modeling, estimation and control for aerial grasping and manipulation," in *IROS*, pp. 2668–2673, IEEE, 2011.
- [2] A. Albers, S. Trautmann, T. Howard, T. A. Nguyen, M. Frietsch, and C. Sauter, "Semiautonomous flying robot for physical interaction with environment," in *Robotics, Automation and Mechatronics*, 2010.
- [3] P. Pounds, D. R. Bersak, and A. M. Dollar, "Grasping from the air: Hovering capture and load stability," in *ICRA*, pp. 2491–2498, IEEE, 2011.
- [4] V. Lippiello and F. Ruggiero, "Exploiting redundancy in cartesian impedance control of uavs equipped with a robotic arm," in *Proceedings of the 2012 IEEE/RSJ International Conference on Intelligent Robots and Systems*, 2012.
- [5] C. M. Korpela, T. W. Danko, and P. Y. Oh, "MM-UAV: Mobile manipulating unmanned aerial vehicle," *Journal of Intelligent and Robotic Systems*, vol. 65, no. 1-4, pp. 93–101, 2012.
- [6] K. Kondak, A. Ollero, I. Maza, K. Krieger, A. Albu-Schäffer, M. Schwarzbach, and M. Laiacker, *Handbook of Unmanned Aerial Vehicles*, ch. Unmanned Aerial Systems Physically Interacting with the Environment. Load Transportation, Deployment and Aerial Manipulation. Berlin, Germany: Springer-Verlag, 2013.
- [7] F. Huber, K. Kondak, K. Krieger, D. Sommer, M. Schwarzbach, M. Laiacker, I. Kossyk, and A. Albu-Schäffer, "First analysis and experiments in aerial manipulation using fully actuated redundant robot arm," in *IEEE/RSJ International Conference on Intelligent Robots and Systems*, 2013.
- [8] A. Albu-Schäffer, C. Ott, and G. Hirzinger, "A unified passivity-based control framework for position, torque and impedance control of flexible joint robots," *The International Journal of Robotics Research*, vol. 26, no. 1, pp. 23–39, 2007.
- [9] C. Ott, *Cartesian Impedance Control of Redundant and Flexible-Joint Robots*. Berlin, Germany: Springer-Verlag, 2008.
- [10] M. Bernard, K. Kondak, I. Maza, and A. Ollero, "Autonomous transportation and deployment with aerial robots for search and rescue missions," *Journal of Field Robotics*, vol. 28, no. 6, pp. 914–931, 2011.
- [11] K. Kondak, M. Bernard, N. Meyer, and G. Hommel, "Autonomously flying vtol-robots: Modeling and control," in *International Conference on Robotics and Automation, ICRA*, IEEE, 2007.